X-615-68-303
PREPRINT

AN ION-EXOSPHERE WITH VARIABLE CONDITIONS AT THE BAROPAUSE

R. E. HARTLE

AUGUST 1968

GSFC — GODDARD SPACE FLIGHT CENTER —
GREENBELT, MARYLAND

X-615-68-303
PREPRINT

AN ION-EXOSPHERE WITH VARIABLE CONDITIONS AT THE BAROPAUSE

R. E. Hartle

August 1968

Goddard Space Flight Center
Greenbelt, Maryland

CONTENTS

AN ION-EXOSPHERE WITH VARIABLE CONDITIONS AT THE BAROPAUSE

R. E. Hartle
Laboratory for Space Sciences,
NASA-Goddard Space Flight Center,
Greenbelt, Maryland

ABSTRACT

The model ion-exosphere of Eviatar, Lenchek and Singer for a nonrotating planet with a static, centered-dipole magnetic field is generalized by permitting the density and temperature to vary over the baropause. In particular, the density and/or temperature are allowed to differ at the conjugate magnetic field points of the baropause. For this case, the ion and electron velocity-distribution functions, satisfying the Vlasov equations in the drift approximation, are constructed. Then, the species densities are determined from the distributions and compared with the corresponding results of Eviatar et. al. for the case of uniform density and temperature at the baropause. In addition, the particle current densities, pressures and temperatures are derived.

I. Introduction

A model ion-exosphere for a nonrotating planet with a static, centered-dipole magnetic field was constructed by Eviatar, Lenchek and Singer.[1] This theory has been a useful step towards a better understanding of planetary atmospheres (see, e.g., the review articles by S. J. Bauer[2] and F. L. Scarf[3] for discussions of applications and further references to work on this subject). The salient features and assumptions made in the model of Eviatar et. al. are as follows: The base or baropause is an imaginary surface where the particle mean free path is of the same order of magnitude as its path length in the exosphere. The ion-exosphere is the region exterior to the baropause where collisions are so infrequent that they can be ignored. Within the baropause lies the barosphere where collisions are so frequent that the ion and electron velocity distributions are Maxwellian and have equal temperatures. All charged particles that populate the exosphere have emerged from the barosphere. Such complicating factors as the presence of neutral particles, ion creation and loss and interaction with interplanetary plasma are neglected. The following analysis is based on the same simplifying assumptions.

In addition to these assumptions, Eviatar et. al. simplified the problem by requiring the baropause to be a spherical surface on which the density and temperature are constant. A more general baropause, of course, would consist of a nonspherical surface over which the density and temperature can vary. In the following treatment the density and temperature are allowed to vary over the class of baropause surfaces that are symmetric about the magnetic equator.

For this case, the corresponding density, pressure, temperature, etc. are derived for both species of an exosphere composed of fully ionized hydrogen.

When the density and temperature are nonuniform on the baropause, currents may flow from one hemisphere of the exosphere to the other leading to the possibility of charge buildup in the barosphere. To avoid the complication arising from the formation of corresponding plasma sheaths at the baropause, it is assumed that either the currents entering or leaving the exosphere are connected in the barosphere to form closed loops or that the barosphere acts as a combination source and sink for current. Furthermore, only those cases of weak electric current are considered so that the resulting induced magnetic field can be ignored relative to the main dipole field.

Following Eviatar et. al., the particle trajectories in the ion-exosphere are determined by the usual nonrelativistic drift approximation. This restricts the exospheric models considered to those with strong magnetic fields such that the average Larmor radius is much smaller than the typical scale length. This also requires the nonmagnetic forces to be weak so that the change in particle velocity over a cyclotron period is small relative to the average velocity. Furthermore, the particle drift across magnetic field lines is assumed negligible compared with the average particle path length in the exosphere.

Subject to the given boundary conditions, explicit solutions of the Vlasov equations in the drift approximation for the proton and electron velocity-distribution functions f^+ and f^- (superscripts + and - refer to protons and electrons throughout), respectively, are constructed in Section II. The electrostatic

field is assumed to be the usual polarization field which is then shown to be self-consistent with the resulting Poisson equation in Section III, where the species densities are derived. The corresponding longitudinal particle current densities and longitudinal and transverse pressures for each species are also obtained in Section IV.

The cgs electromagnetic system of units is used throughout this work.

II. Velocity-Distribution Functions: Drift Approximation

In order to represent the boundary conditions, first consider the magnetic dipole field line directed from 1 to m in Figure 1. The magnetic field $\vec{B}$ is centered about the origin O of the planet and has an equatorial plane passing through the line O-m. The baropause surface, assumed continuous and symmetric about the equatorial plane for simplicity, crosses the field line at points 1 and 2 where the radial distances $|\vec{r}_1| = |\vec{r}_2|$ and the latitude angles $\lambda_1 = -\lambda_2$. Unless otherwise noted, subscripts 1 and 2 hereafter refer to quantities evaluated at the conjugate points $\vec{r}_1$ and $\vec{r}_2$, respectively. The length s measured from point 1 in the direction of the magnetic field is given by

$$s = (r_1/2\cos^2\lambda_1)\left[Y(\lambda_1)\sin\lambda_1 - Y(\lambda)\sin\lambda + 3^{-1/2}\ln\left(\frac{3^{1/2}\sin\lambda_1 + Y(\lambda_1)}{3^{1/2}\sin\lambda + Y(\lambda)}\right)\right] \tag{1}$$

in terms of $Y(\lambda) = (1 + 3\sin^2\lambda)^{1/2}$ and the latitude angle λ entering the relation

$$r = r_1 \cos^2\lambda/\cos^2\lambda_1 , \tag{2}$$

where r is the radial distance to the magnetic field line. Then, at $\vec{r}_1$ and $\vec{r}_2$ the emerging distributions have the Maxwellian forms

$$f^{\pm} = \beta_1^{\pm} \exp\left[-m^{\pm} v^2/2kT_1\right] \text{ for } \vec{v}\cdot\vec{B}(\vec{r}_1) > 0 , \tag{3a}$$

and

$$f^{\pm} = \beta_2^{\pm} \exp\left[-m^{\pm} v^2/2kT_2\right] \text{ for } \vec{v}\cdot\vec{B}(\vec{r}_2) < 0, \tag{3b}$$

respectively, where k is Boltzmann's constant, $m^{\pm}$ are the component masses and v is the magnitude of their respective velocities $\vec{v}$. The quantities $\beta_j^{\pm}$ for j = 1,2 equal $N_j (m^{\pm}/2\pi kT_j)^{3/2}$ in terms of the baropause densities N_j and temperatures T_j (the superscripts + and - have been dropped since $N_j^+ = N_j^-$ and $T_j^+ = T_j^-$).

The kinetic equation in the drift approximation (or guiding center approximation) can be obtained by first introducing the drift variables $(\vec{R}, v_\perp, v_{||})$ into the Vlasov equations for $f^{\pm}$, where $\vec{R}$ is the position of the guiding center and $v_\perp$ and $v_{||}$ are the components of velocity transverse and longitudinal to the magnetic field

$$\vec{B} = 3\frac{\vec{\kappa}\cdot\vec{r}}{r^5}\vec{r} - \frac{\vec{\kappa}}{r^3} \tag{4}$$

in terms of the magnetic moment $\vec{\kappa}$. Then, expanding the resulting kinetic equations in powers of the ratios $R_B^{\pm}/L$, the Larmor radii to the scale length, one obtains the kinetic equations for $f_0^{\pm}$ of $f^{\pm} = f_0^{\pm} + (R_B^{\pm}/L) f_1^{\pm} + (R_B^{\pm}/L)^2 f_2^{\pm} + \ldots$ which are independent of the Larmor phase. Upon neglecting terms corresponding to drift across magnetic field lines and dropping the subscript zero, the steady state kinetic equations for $f_0^{\pm}$ are[4,5]

$$v_{||}\frac{\partial f^{\pm}}{\partial s} - \frac{1}{m^{\pm}}\left(\frac{\partial V^{\pm}}{\partial s} + \frac{m^{\pm} v_\perp^2}{2B}\frac{\partial B}{\partial s}\right)\frac{\partial f^{\pm}}{\partial v_{||}} + \frac{v_{||} v_\perp}{2B}\frac{\partial B}{\partial s}\frac{\partial f^{\pm}}{\partial v_\perp} = 0 \tag{5}$$

where B is the magnitude of the magnetic field and the potential energies $V^{\pm}$ for the two species are given by

$$V^{\pm} = m^{\pm}\varphi_g \pm e\varphi_e \tag{6}$$

in which e is the electronic charge and

$$\varphi_g = -GM/r \tag{7}$$

is the gravitational potential in terms of the gravitational constant G and the radial position r from the center of the planet of mass M. The electrostatic potential is taken to be the usual polarization potential of Pannekoek[6] and Rosseland,[7] namely $\varphi_e = -(m^+ - m^-)\,\varphi_g/2e$, which is shown to be self-consistent with Poisson's equation in Section III. Accordingly,

$$V^+ = V^- = (m^+ + m^-)\,\varphi_g/2 \equiv V \tag{8}$$

and the nonmagnetic force $\vec{F} = -\nabla V$ is the same on an electron and proton. In this case, the drift terms $\pm(\vec{F} \times \vec{B}/eB^2)\cdot\nabla f^\pm$ ignored in Eqs. (5) can be approximated by $|\vec{F}|\, f^\pm/eBL_\perp \doteq m^+MGf^\pm/2r^2\, eBL_\perp$ in terms of the transverse scale length $L_\perp$. Then, the neglect of the drift terms relative to those given, say $v_{||}\,\partial f^\pm/\partial s \sim v_{th}^{\pm} f^\pm/L_{||}$ in terms of the thermal velocities $v_{th}^{\pm} = (3kT^\pm/m^\pm)^{1/2}$ and the longitudinal scale $L_{||}$, is justified when the planetary models considered satisfy $Bev_{th}^{+}/|\vec{F}| \gg 1$ or equivalently, $B \gg 1.1 \times 10^{-16} M/r^2\,(T^+)^{1/2}$, assuming $L_\perp/L_{||}$ is of order unity.

By the method of characteristics,[8] the general solutions of Eqs. (5) consist of arbitrary functions of the integration constants $E^\pm$ and $\mu^\pm$ of the corresponding characteristic equations; that is, $f^\pm = F^\pm(E^\pm, \mu^\pm)$, where

$$E^\pm = m^\pm v^2/2 + V, \tag{9a}$$

$$\mu^\pm = m^\pm v_\perp^2/2B, \tag{9b}$$

and $F^\pm$ are arbitrary functions of their arguments. One notes that $E^\pm$ are the particle energies with $v^2 = v_\perp^2 + v_{||}^2$ and $\mu^\pm$ are their magnetic moments or first adiabatic invariants.

The potential energies and the magnetic field are symmetric about the equator and their magnitudes monotonically decrease from the baropause to a minimum at point m. Accordingly, a particle emerging from the barosphere at point 1 and also passing point m will enter the barosphere at point 2 and vice versa. Since the particles populating the exosphere have emerged from either points 1 or 2, they must have $E^{\pm}$ and $\mu^{\pm}$ satisfying either

$$\alpha_1^{\pm} \equiv E^{\pm} - \mu^{\pm} B_1 - V_1 > 0 \tag{10a}$$

or

$$\alpha_2^{\pm} \equiv E^{\pm} - \mu^{\pm} B_2 - V_2 > 0 , \tag{10b}$$

respectively, and those particles passing point m must also satisfy

$$\alpha_m^{\pm} \equiv E^{\pm} - \mu^{\pm} B_m - V_m > 0 , \tag{11}$$

where the quantities with subscript m are evaluated at point m. Due to the symmetry of the system $\alpha_1^{\pm} = \alpha_2^{\pm}$ for a given $E^{\pm}$ and $\mu^{\pm}$; however, the separate identification between $\alpha_1^{\pm}$ and $\alpha_2^{\pm}$ is retained for generality.

A principle noted by Aamodt and Case[9] in connection with the neutral exosphere problem is applied to construct the component distribution functions. That is, $f^{\pm}$ need not be continuous or single-valued functions of their arguments. With this in mind, consider the parts $F_1^{\pm}$ of the distribution functions $f^{\pm}$ due only to particles that have emerged from point 1. To insure that the orbits of these particles intersect point 1, $F_1^{\pm}$ must vanish when $\alpha_1^{\pm} < 0$. Particles passing point m from point 1 will not return to point 1; therefore, in segment I, between points 1 and m, $F_1^{\pm}$ must vanish when $v_{||} < 0$ and $\alpha_m^{\pm} > 0$. Accordingly, the distribution functions $F_1^{\pm}$ in segment I satisfying these conditions and Eq. (3a) are

$$F_1^{\pm} = \beta_1^{\pm} \exp\left[-(E^{\pm} - V_1)/kT_1\right] S(\alpha_1^{\pm}) \left[1 - S(\alpha_m^{\pm}) S(\epsilon_2 v_{||})\right] , \tag{12}$$

where the unit step function

$$S(x) = \begin{cases} 1 & x > 0 \\ 0 & x < 0 \end{cases} \tag{13}$$

and $\epsilon_j = (-1)^{j+1}$ for $j = 1,2$. The particles emerging from point 1 and passing into segment II, between points m and 2, satisfy the conditions $\alpha_1^{\pm} > 0$, $\alpha_m^{\pm} > 0$ and $v_{||} > 0$. Due to the symmetry of the electric and magnetic fields, this class of particles with $\vec{v} \cdot \vec{B} > 0$ has the same velocity distribution at conjugate magnetic field points in segments I and II. Then, in segment II

$$F_1^{\pm} = \beta_1^{\pm} \exp[-(E^{\pm} - V_1)/kT_1] S(\alpha_1^{\pm}) S(\alpha_m^{\pm}) S(\epsilon_1 v_{||}) . \tag{14}$$

Again, due to the symmetry of the system, those parts $F_2^{\pm}$ of $f^{\pm}$ corresponding to particles emerging from point 2 are obtained for segments I and II by simply permuting the subscripts from 1 to 2 and 2 to 1 in Eqs. (14) and (12), respectively. Altogether, the total distribution functions in segment I are

$$\begin{aligned} f^{\pm} = {} & \beta_1^{\pm} \exp[-(E^{\pm} - V_1)/kT_1] S(\alpha_1^{\pm}) \; [1 - S(\alpha_m^{\pm}) S(\epsilon_2 v_{||})] \\ & + \beta_2 \exp[-(E^{\pm} - V_2)/kT_2] S(\alpha_2^{\pm}) S(\alpha_m^{\pm}) S(\epsilon_2 v_{||}) , \end{aligned} \tag{15}$$

satisfying the above requirements and the boundary condition of Eq. (3a). The total distribution functions in segment II are obtained by permuting the subscripts from 1 to 2 and 2 to 1 in Eqs. (15). At their common point m, the total distributions for segments I and II become

$$f^{\pm} = \{\beta_1^{\pm} \exp(-Q^{\pm}/kT_1) S(v_{||}) + \beta_2^{\pm} \exp(-Q^{\pm}/kT_2) S(-v_{||})\} S(\alpha_1^{\pm}) , \tag{16}$$

where $Q^{\pm} = m^{\pm} v^2/2 - (V_1 - V_M)$. In the symmetric case when $N_1 = N_2$ and $T_1 = T_2$, the total distribution functions have the same form in segments I and II, given by

$$f^{\pm} = \beta_1^{\pm} \exp[-(E^{\pm} - V_1)/kT_1] S(\alpha_1^{+}) \tag{17}$$

from which the zeroth order velocity moment is shown below to be identical to the density distribution derived by Eviatar et. al.

The question arises whether or not the kinetic Eqs. (5) are satisfied by $f^{\pm}$ of Eqs. (15) and the corresponding $f^{\pm}$ of segment II since they are not strictly functions of the constants $E^{\pm}$ and $\mu^{\pm}$ (due to their dependance on $S(\epsilon_j, v_{||})$ for $j = 1,2$). It is worth noting that a similar problem arose in connection with a solution of the collisionless Boltzmann equation obtained by Aamodt and Case[9] for the neutral exosphere. Consider the left-hand sides of Eqs. (5) which reduce to

$$\{\beta_1^{\pm} \exp[-(E^{\pm}-V_1)/kT_1] - \beta_2^{\pm} \exp[-(E^{\pm}-V_2)/kT_2\} S(\alpha_1^{\pm}) S(\alpha_m^{\pm}) \delta(v_{||}) \qquad (18)$$

upon substitution of Eqs. (15), where δ represents the Dirac delta function. As an aid in discussing whether or not this expression vanishes, consider the plots of $\alpha_1^{\pm}$ and $\alpha_m^{\pm}$ versus $\mu^{\pm}$ for $v_{||} = 0$ shown in Figure 2. The intersection point of $\alpha_1^{\pm} = \alpha_m^{\pm}$ (for $v_{||} = 0$) is $\mu^{\pm} = -(V_1 - V_m)/(B_1 - B_m)$ at which point

$$\alpha_1^{\pm} = V\{1 - [(B-B_m)V_1/V + (B_1-B)V_m/V]/[B_1 - B_m]\}. \qquad (19)$$

It can be shown that the term within the curly brackets of Eqs. (19) is greater than zero for $s_1 < s < s_2$ along all field lines corresponding to the range $0 < \lambda_1 < \pi/2$. (To show this, one employs the expression for B obtained from Eq. (4) and V of Eq. (8) in conjunction with the field line coordinate constrained by Eq. (2)). Then, the intersection point $\alpha_1^{\pm} = \alpha_m^{\pm} < 0$ and, referring to Figure 2, either $S(\alpha_1^{\pm}) = 0$ or $S(\alpha_m^{\pm}) = 0$ for $\mu^{\pm} \geq -(V_1 - V_m)/(B_1 - B_m)$ or $0 < \mu^{\pm} \leq -(V_1 - V_m)/(B_1 - B_m)$, respectively. Therefore, expression (18) vanishes and the kinetic equation is satisfied. In an analogous fashion one can show that $f^{\pm}$ for segment II also satisfies the kinetic equation.

In general, the density and temperature vary on the baropause surface. In this case, the parameters N_1, N_2, T_1 and T_2 appearing in Eqs. (15) will be functions of position $\vec{r}$ which reduce to their corresponding boundary values on the

baropause. For example, suppose the variation of density N_1 is prescribed by some function, say $N(\vec{r}_1)$, where the tip of $\vec{r}_1$ defines the baropause surface. Then, the function, say $F(\vec{r})$, replacing N_1 in Eqs. (15) for segment I and N_1 in the corresponding expression for segment II must satisfy $F(\vec{r}_1) = N(\vec{r}_1)$ on the baropause. When the parameters N_1, N_2, T_1 and T_2 are replaced by functions of position, the resulting distribution functions $f^{\pm}$ will not, in general, satisfy the kinetic equations. However, since the kinetic equations are of zero order in $R_B^{\pm}/L$, such a replacement is permissible when the local scale lengths of the functions replacing N_1, N_2, T_1 and T_2 are much larger than the corresponding Larmor radius. In this instance, the kinetic equations remain satisfied to zero order in $R_B^{\pm}/L$.

The effects of rotation, when the ion-exosphere co-rotates with the planet, have been treated by Melrose[10] for the case of uniform density and temperature at the baropause. In this instance, the potential energies $V^{\pm}$ of Eqs. (6) are modified by the addition of the centrifugal potential energies $-m^{\pm}(\vec{\Omega}\times\vec{r})^2/2$ in terms of the angular velocity $\vec{\Omega}$ of the planet. It is worth noting at this point that the above treatment may be generalized to include such rotation when $\vec{\Omega}$ and $\vec{\kappa}$ are parallel or antiparallel. In this case, $V^{\pm}$ is symmetric about the equator when φ_e is symmetric. However, $V^{\pm}$ will not, in general, be monotonic from the baropause to point m. To apply the above procedure, segments I and II must be divided in two parts corresponding to the points where the centrifugal force becomes dominant; i.e., where $\partial V^{\pm}/\partial s$ vanishes. On the other hand, if φ_e is not symmetric then $V^{\pm}$ will not be, as might be the case when the baropause radii $|\vec{r}_1| \neq |\vec{r}_2|$ (not treated here). Further segmentation may then be necessary since the maximum or minimum points of $V^{\pm}$ occurring at the equator in the

symmetric case may be shifted. In each of the above instances, the electrostatic potential may be determined by application of the quasi-neutrality approximation $n^+ = n^-$ or by direct solution of Poisson's equation.

III. Density Distribution

The densities $n^\pm$ of the component guiding centers to zeroth order in $R_B^\pm/L$ are

$$n^\pm = \int f_0^\pm \, d^3 v \tag{20}$$

and, of course, are good approximations to the actual particle density when $R_B^\pm/L \ll 1$. These quadratures on $f^\pm$ of Eqs. (15) for segment I and the corresponding $f^\pm$ for segment II lead to $n^+ = n^-$, in which case Poisson's equation $\nabla^2 \varphi_e = -4\pi c^2 e(n^+ - n^-)$ is identically satisfied to the order considered. Then, omitting the superscripts + and -, the density ratio n/N_1 in segment I is

$$\begin{aligned} n/N_1 = {} & \exp(b_{11})\,[1-(1-\eta)^{1/2}\exp(b_{21})] \\ & -\frac{1}{2}\sum_{j=1}^{2}(-1)^{j+1}\,\delta_j \exp(b_{1j})\,\{\Phi(a_{1j}) - (1-\eta)^{1/2}\exp(b_{2j})\Phi(a_{4j}) \\ & + (\gamma-1)^{1/2}\exp(b_{3j})\,[\psi(a_{2j}) - \psi(a_{3j})]\} \end{aligned} \tag{21}$$

in terms of the complementary error function

$$\Phi(x) = 1 - \left(\frac{4}{\pi}\right)^{1/2}\int_0^x \exp(-t^2)\,dt \tag{22}$$

and a form of Dawson's integral[11]

$$\psi(x) = \left(\frac{4}{\pi}\right)^{1/2}\int_0^x \exp(t^2)\,dt. \tag{23}$$

For $j = 1, 2$, the density ratio $\delta_j = N_j/N_1$ and the arguments appearing in Eq. (21) are given by

$$a_{1j} = [(V_m - V)/kT_j]^{1/2}, \quad a_{2j} = a_{1j}/(\gamma - 1)^{1/2}, \tag{24a,b}$$

$$a_{3j} = \{a_{2j}^2 + (V_1 - V_m)/[(B_1/B_m - 1)kT_j]\}^{1/2}, \tag{24c}$$

$$a_{4j} = \{a_{1j}^2 + (\gamma - 1)(V_1 - V_m)/[(B_1/B_m - 1)kT_j]\}^{1/2} (1 - \eta)^{-1/2}, \tag{24d}$$

$$b_{1j} = (V_1 - V)/kT_j, \quad b_{2j} = \eta b_{1j}/(1 - \eta), \quad b_{3j} = -\gamma a_{2j}^2 \tag{24e,f,g}$$

in terms of the dipole field ratios

$$\eta \equiv B/B_1 = (\cos\lambda_1/\cos\lambda)^6 [(1+3\sin^2\lambda)/(1+3\sin^2\lambda_1)]^{1/2}, \tag{25a}$$

$$\gamma \equiv B/B_m = (1+3\sin^2\lambda)^{1/2}/\cos^6\lambda. \tag{25b}$$

The density ratio n/N_1 in segment II is obtained by permuting the subscripts 1 to 2 and 2 to 1 on the right-hand side of Eq. (21) (only the right most subscript on the double subscripted variables) but not on the denominator of $\delta_j = N_j/N_1$. In the symmetric case, when $N_1 = N_2$ and $T_1 = T_2$, the summations in the expressions for n/N_1 vanish. Thus, the density ratios n/N_1 in segments I and II have the same form given by

$$n/N_1 = \exp(b_{11})[1-(1-\eta)^{1/2} \exp(b_{21})] \tag{26}$$

in consonance with the result of Eviatar et. al. for this case. This relation can, of course, be obtained by direct integration of Eqs. (17) for $f^{\pm}$. As noted by Eviatar et. al., the term in square brackets reduces the density below that of the simple barometric law given by $n/N_1 = \exp(b_{11})$.

To exhibit some of the main differences in the density distribution along a field line between the symmetric model of Eq. (26) and the asymmetric model of Eq. (21) for segment I along with the expression corresponding to segment II, consider the graphs of n/N_1 versus latitude angle λ shown in Figures 3 and 4. In correspondence with some of the numerical examples presented by Eviatar et. al., the baropause radii $r_1 = r_2$ were chosen to be 1.1 earth radii at latitude

angles $\lambda_1 = \lambda_2 = 45°$ and M was taken to be the mass of earth. The solid lines in Figures 3 and 4 correspond to the symmetric case $N_1 = N_2$ and $T_1 = T_2 = 1500°K$. To simplify the task of interpretation, only the effects of varying the density ratio N_2/N_1, keeping $T_1 = T_2 = 1500°K$, are considered in Figure 3. That is, the dashed lines in Figure 3 correspond to $N_2 = 0.5N_1$ and $N_2 = 2N_1$ for $T_1 = T_2 = 1500°K$. On the other hand, in Figure 4, only the temperature T_2 is changed with respect to the symmetric example, where the cases $T_2 = 0.5T_1 = 750°K$ and $T_2 = 2T_1 = 3000°K$ for $N_1 = N_2$ are shown by dashed lines. The ratios N_2/N_1 and T_2/T_1 were chosen only to simplify the presentation of the results and may not be useful to any model of an actual exosphere.

Relative to the symmetric case, one can observe in Figure 3 that the density is reduced in both segments I and II when the density is reduced at point 2 from the value of the symmetric example. This can be viewed as a result of the reduction in the particle injection rate into the system. The density reduction in segment I corresponds to a reduction in those particles that emerge from point 2 and pass into segment I. However, at all conjugate field points, there is a greater reduction of density in segment II than segment I. This reflects the fact that a greater fraction of the particles emerging from point 2 remain in segment II than pass into segment I. Converse comparisons can be made when the density is increased at point 2 above the value of the symmetric example. Further, when $N_2 = 0.5N_1$, it can be noted that at point 1 (point 2) the density n_1 (n_2) is less (greater) than the density N_1 (N_2) just below the baropause. This decrease (increase) at point 1 (point 2) occurs because more (fewer) particles are emitted at point 1 (point 2) which pass into segment II (segment I) – not returning – than are emitted at point 2 (point 1) which pass into segment I (segment II). A similar

observation can be made for the case $N_2 = 2N_1$. As noted by Herring and Kyle[12] in connection with the neutral exosphere problem, such discontinuities would be removed in a more realistic theory where the sharp boundaries would be replaced by diffuse zones which account for a gradual decrease in collision frequency.

When the temperature of the symmetric model is reduced at point 2, reducing the particle injection rate, one observes, in Figure 4, that the total number of particles in the system is, of course, reduced. The decrease in temperature at point 2 leads to a decrease in the high energy tail of the velocity distribution of emergent particles with a corresponding increase in the number of low energy particles. This results in a relative increase in the number of particles populating low altitudes of segment II along with a corresponding decrease at high altitudes. The reduction of the number of particles in the high energy tail also results in fewer particles being able to pass over the peak of the potential barrier at point m, leading to the density decrease in segment I. Similar comparisons can be made for the case $N_2 = 2N_1$. As in the asymmetric examples of Figure 3, one observes analogous density discontinuities due, again, to the net flow of particles from one segment to the other.

The above examples are not intended to represent any actual planetary ion-exosphere but only to indicate some of the differences between symmetric and asymmetric models in the simplest manner. Only one field line was considered because the salient differences between the two models are essentially the same on other field lines.

IV. Higher Order Velocity Moments

The mean velocity, pressure, temperature, etc. of each component to zeroth order in $R_B^{\pm}/L$ are functions of one or more of the velocity moments

$$n\langle v_\sigma{}^p\rangle^{\pm} = \int v_\sigma{}^p f_0^{\pm} d^3v \tag{27}$$

of order $p = 0, 1, 2, \ldots$, where σ corresponds to either the transverse $\perp$ or longitudinal $\parallel$ symbol. Referring to the distribution functions $f^{\pm}$ of Eqs. (15) for segment I, one notes that the velocity moments can be expressed as

$$n\langle v_\sigma{}^p\rangle^{\pm} = I_1^{\pm}(p,\sigma) - K_1^{\pm}(p,\sigma,\epsilon_2) + K_2^{\pm}(p,\sigma,\epsilon_2) \tag{28}$$

in terms of the quadratures

$$I_j^{\pm}(p,\sigma) = \beta_j^{\pm} \int v_\sigma{}^p \exp\left[-(E^{\pm} - V_1)/kT_j\right] S(\alpha_1^{\pm}) d^3v \tag{29a}$$

$$K_j^{\pm}(p,\sigma,\epsilon_\ell) = \beta_j^{\pm} \int v_\sigma{}^p \exp\left[-(E^{\pm} - V_1)/kT_j\right] S(\alpha_1^{\pm}) S(\alpha_m^{\pm}) S(\epsilon_\ell v_{\parallel}) d^3v \tag{29b}$$

for $j = 1, 2$ and $\ell = 1, 2$. Permutation of all subscripts on the right-hand side of Eqs. (28) from 1 to 2 and 2 to 1 leads to the velocity moments in segment II. The first terms on the right-hand sides of Eqs. (28) can be identified as the velocity moments resulting in the symmetric model; i.e., when $N_1 = N_2$ and $T_1 = T_2$ the velocity moments become $I_1^{\pm}(p,\sigma)$ since $K_1(p,\sigma,\epsilon_\ell) = K_2(p,\sigma,\epsilon_\ell)$ (the subscripts 1 and 2 are superfluous in this case). With this in mind, one may identify the second and third terms as those affecting the change in the moments of the symmetric model when $N_2 \neq N_1$ and/or $T_2 \neq T_1$. An analogous identification of the terms of the velocity moments of segment II can be made.

The transverse particle current densities $n\langle v_\perp\rangle^{\pm}$ vanish to zeroth order in $R_B^{\pm}/L$; however, in general, the longitudinal current densities $n\langle v_{\parallel}\rangle^{\pm}$ are finite

to this order. The longitudinal current densities are the same at conjugate field points in segments I and II respectively. Accordingly,

$$n\langle v_{||}\rangle^{\pm} = \gamma \sum_{j=1}^{2} \mathcal{E}_j N_j (kT_j/2\pi m^{\pm})^{1/2} \exp(b_{4j}) [1-(1-B_m/B_1)\exp(b_{5j})] \qquad (30)$$

in segments I and II, where

$$b_{4j} = (V_1 - V_m)/kT_j, \quad b_{5j} = b_{4j}/(B_1/B_m - 1) \qquad (31a,b)$$

are constants on a given field line. Since the cross-sectional area of a flux tube is proportional to 1/B and $n\langle v_{||}\rangle^{\pm}$ = constant $B/(m^{\pm})^{1/2}$, one notes that the particle currents passing various points on the same flux tube are constant; i.e., $(\partial/\partial s)(n\langle v_{||}\rangle^{\pm}/B) = 0$. The longitudinal current densities vanish in the symmetrical model and also when the density and temperature at points 1 and 2 satisfy the constraint

$$N_1/N_2 = (T_1/T_2)^{1/2} \exp(b_{41} - b_{42}) \left[\frac{1-(1-B_m/B_1)\exp(b_{51})}{1-(1-B_m/B_1)\exp(b_{52})}\right] . \qquad (32)$$

It is worth noting that this expression is simply $N_1/N_2 = (T_1/T_2)^{1/2}$ to zeroth order in $(V_1 - V_m)/kT_j$ when $|(V_1 - V_m)/kT_j| << 1$ for j = 1, 2.

When there is a net particle flow from one hemisphere to the other, there will always be an electric current since $\langle v_{||}\rangle^{-}/\langle v_{||}\rangle^{+} = (m^{+}/m^{-})^{1/2}$. These currents must be weak in the sense that the induced field $\vec{B}'$ satisfies $|\vec{B}'|/|\vec{B}| << 1$. From Ampere's law, the magnitude of the induced field B' can be approximated in terms of its scale length L' by $B' \sim 4\pi en|\langle v_{||}\rangle^{-}|L'$. Then, requiring $B'/B << 1$ and using the property $n\langle v_{||}\rangle^{-}/B$ = constant, one has

$$L'/B_1 << 1/(4\pi en|\langle v_{||}\rangle^{-}|)_{\vec{r}=\vec{r}_1} \qquad (33)$$

which relates a necessary restriction on the ion-exospheric models considered.

For the asymmetric examples considered in the previous section, the particle current densities at $\vec{r}_1$ are: $2.6 \times 10^6 N_1$ and $-3.4 \times 10^6 N_1$ $cm^{-2} sec^{-1}$ for $T_2 = 0.5T_1 = 750°K$ and $T_2 = 2T_1 = 3000°K$ when $N_1 = N_2$; $2.0 \times 10^6 N_1$ and $-3.9 \times 10^6 N_1$ $cm^{-2} sec^{-1}$ for $N_2 = 0.5N_1$ and $N_2 = 2N_1$ when $T_1 = T_2 = 1500°K$. When a conservative value $n\langle v_{||} \rangle^- \approx 5 \times 10^6 N_1$ is assumed $L'/B_1 N_1 << 10^{12}$ cm^4 $gauss^{-1}$. Then, for these cases, the class of models that can be treated by the above are restricted by $B_1 N_1 >> 10^{-3}$ gauss cm^{-3} when a conservative value $L' \approx 10^9$ cm (the approximate length of a field line) is assumed.

To zeroth order in $R_B^{\pm}/L$, the transverse and longitudinal pressures $p_\perp^{\pm}$ and $p_{||}^{\pm}$, respectively, are defined in terms of the velocity moments by

$$p_\perp^{\pm} = \frac{1}{2} m^{\pm} \int v_\perp^2 \, f_0^{\pm} \, d^3 v = \frac{1}{2} m^{\pm} n \langle v_\perp^2 \rangle^{\pm} \tag{34a}$$

$$p_{||}^{\pm} = m^{\pm} \int (v_{||} - \langle v_{||} \rangle^{\pm})^2 f_0^{\pm} \, d^3 v = m^{\pm} n \left[\langle v_{||}^2 \rangle^{\pm} - (\langle v_{||} \rangle^{\pm})^2 \right] \tag{34b}$$

and, for the symmetric case, with $N_1 = N_2$ and $T_1 = T_2$, they become

$$p_\perp = N_1 k T_1 \exp(b_{11}) \left[1 - (1-\eta)^{1/2} \left(1 + \frac{1}{2}\eta - b_{21} \right) \exp(b_{21}) \right], \tag{35a}$$

$$p_{||} = N_1 k T_1 \exp(b_{11}) \left[1 - (1-\eta)^{3/2} \exp(b_{21}) \right], \tag{35b}$$

explicitly, in both segments I and II. The superscripts have been omitted since the species pressures are equal on the symmetric model. The transverse and longitudinal pressures for the more general case $N_1 \neq N_2$ and/or $T_1 \neq T_2$ are given in the Appendix for completeness. Since the difference $(p_{||} - p_\perp)$ on the symmetric model can be expressed as

$$p_{||} - p_\perp = N_1 k T_1 (1-\eta)^{1/2} \left(\frac{3}{2}\eta - b_{21} \right) \exp(b_{21}/\eta), \tag{36}$$

one notes that $p_{||} > p_{\perp}$ at all points $s_1 < s < s_2$ and that $p_{||} = p_{\perp} = N_1 k T_1$ at points 1 and 2, their isotropic value just below the baropause. Furthermore, one can show that both the transverse and longitudinal pressures decrease, along a flux tube, from their values at the baropause to a minimum at the equator.

The transverse and longitudinal temperatures $T_{\perp}$ and $T_{||}$, respectively, fixed by $p_{\perp} = nkT_{\perp}$ and $p_{||} = nkT_{||}$, can be written as

$$T_{\perp} = T_1 \left[1 - \frac{(1-\eta)^{1/2} \left(\frac{1}{2}\eta - b_{21} \right) \exp(b_{21})}{1-(1-\eta)^{1/2} \exp(b_{21})} \right] \tag{37a}$$

$$T_{||} = T_1 \left[\frac{1-(1-\eta)^{3/2} \exp(b_{21})}{1-(1-\eta)^{1/2} \exp(b_{21})} \right] \tag{37b}$$

on combining Eqs. (26) and (35). It is clear that $T_{\perp}$ is less than its value T_1 at the baropause. On the other hand, $T_{||}$ increases along a flux tube from T_1 at the baropause to a maximum at the equator.

Acknowledgments

The author would like to thank Drs. S. J. Bauer, S. Chandra and E. J. R. Maier for helpful discussions during the course of this investigation.

Appendix

The transverse and longitudinal pressures on the assymetric model are obtained by carrying out the operations of Eqs. (34a) and (34b), respectively, on f^+ of Eqs. (15) for segment I and the corresponding $f^\pm$ for segment II. Accordingly, for segment I, one has

$$
\begin{aligned}
p_\perp = {} & N_1 kT_1 \exp(b_{11}) \left[1-(1-\eta)^{1/2}\left(1+\frac{1}{2}\eta-b_{21}\right)\exp(b_{21})\right] \\
& + \frac{1}{2}\sum_{j=1}^{2}(-1)^{j+1} N_j kT_j \Bigg\{\Phi(a_{1j}) \\
& - (1-\eta)^{1/2}\exp(b_{2j})\left[\left(1+\frac{1}{2}\eta-b_{2j}\right)\Phi(a_{4j})+\pi^{-1/2}\eta a_{4j}\exp(-a_{4j}^2)\right] \\
& + (\gamma-1)^{1/2}\exp(b_{3j})\left[\left(1+\frac{1}{2}\gamma-b_{3j}\right)\{\psi(a_{2j})-\psi(a_{3j})\}\right. \\
& \left.\left. - \pi^{-1/2}\gamma\{a_{2j}\exp(a_{2j}^2)-a_{3j}\exp(a_{3j}^2)\}\right]\right\}
\end{aligned}
\tag{A1}
$$

$$
\begin{aligned}
p_{||} = {} & N_1 kT_1 \exp(b_{11})\left[1-(1-\eta)^{3/2}\exp(b_{21})\right] - m^\pm n(\langle v_{||}\rangle^\pm)^2 \\
& + \frac{1}{2}\sum_{j=1}^{2}(-1)^{j+1} N_j kT_j \Bigg\{\Phi(a_{1j}) + \left(\frac{4}{\pi}\right)^{1/2} a_{1j}\exp(-a_{1j}^2) \\
& - (1-\eta)^{3/2}\exp(b_{2j})\left[\Phi(a_{4j}) + \left(\frac{4}{\pi}\right)^{1/2} a_{4j}\exp(-a_{4j}^2)\right] \\
& - (\gamma-1)^{3/2}\exp(b_{3j})\left[\psi(a_{2j})-\psi(a_{3j})-\left(\frac{4}{\pi}\right)^{1/2} a_{2j}\exp(a_{2j}^2)\right. \\
& \left.\left. + \left(\frac{4}{\pi}\right)^{1/2} a_{3j}\exp(a_{3j}^2)\right]\right\}
\end{aligned}
\tag{A2}
$$

where the superscripts have been omitted since the species pressures are equal (one notes, on combining Eqs. (21) and (30), that the second term of Eq. (A2) is independent of particle type). The corresponding pressures in segment II are obtained by permuting the subscripts 1 to 2 and 2 to 1 on the right-hand sides of Eqs. (A1) and (A2) (only the right most subscript on the double subscripted variables).

References

1. A. Eviatar, A. M. Lenchek and S. F. Singer, Phys. Fluids 7, 1775 (1964).

2. S. J. Bauer, "Handbuch d. Physik" (Springer-Verlag, Vienna, in press), Vol. 4914.

3. F. L. Scarf, "Advances in Plasma Physics" (Interscience Publishers, New York, in press), Vol. I.

4. R. S. Sagdeyev, B. B. Kadomtsev, L. I. Rudakov and A. A. Vedyonov, "Proceedings of the Second United Nations International Conference on the Peaceful Uses of Atomic Energy" (United Nations, Geneva, 1958), Vol. 31, pp. 151, 152.

5. D. V. Sivukhin, "Reviews of Plasma Physics" (Consultants Bureau, New York, 1965), Vol. I, pp. 1-104.

6. A. Pannekock, Bull. Astron. Inst. Netherlands 1, 107 (1922).

7. S. Rosseland, Monthly Notices Roy. Astron. Soc. 84, 720 (1924).

8. R. Courant and D. Hilbert, "Methods of Mathematical Physics (Interscience Publishers, New York, 1962), Vol. II, pp. 1-153.

9. R. E. Aamodt and K. M. Case, Phys. Fluids 5, 1019 (1962).

10. D. B. Melrose, Planet. Space Sci. 15, 381 (1967).

11. J. C. P. Miller, "Handbook of Mathematical Functions" (U. S. Government Printing Office, Washington, D. C., 1964), p. 692.

12. J. Herring and J. Kyle, J. Geophys. Res. 66, 1980 (1961).

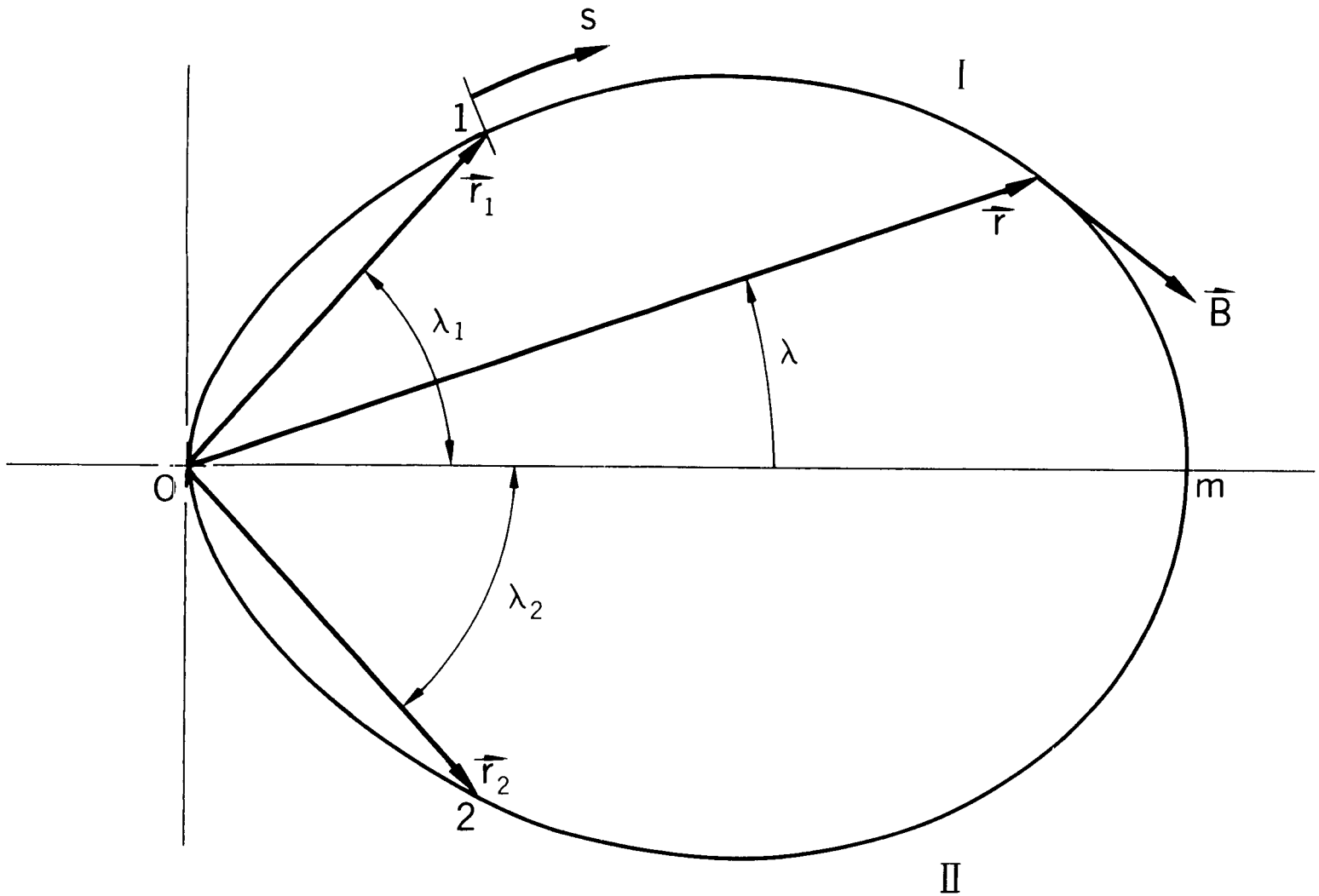

Figure 1–Coordinates of a magnetic dipole field line.

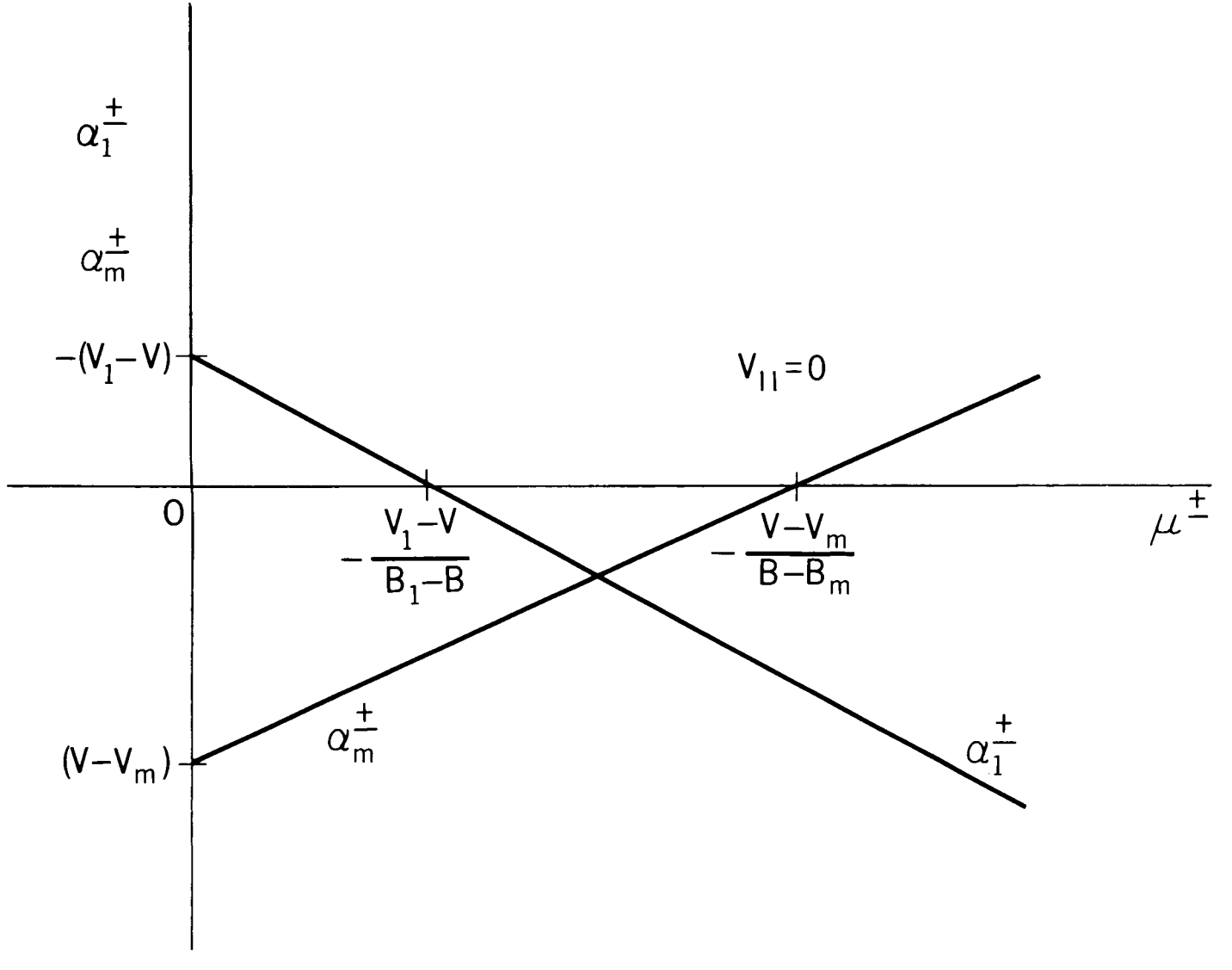

Figure 2–The arguments $\alpha_l^{\pm}$ and $\alpha_m^{\pm}$ of the step functions versus $\mu^{\pm}$ when $v_{ll} = 0$.

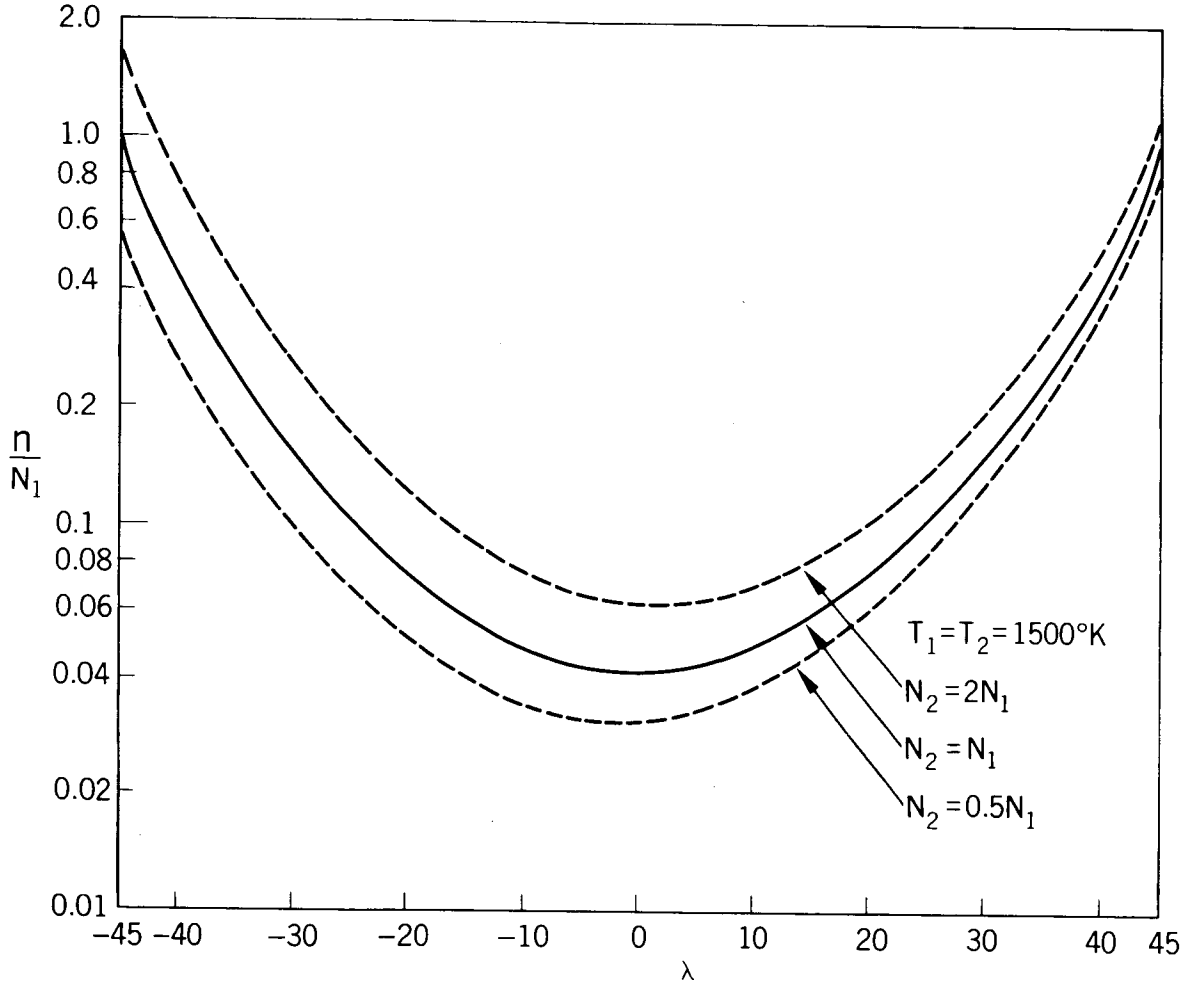

Figure 3–Density ratio n/N_1 versus latitude angle λ along a magnetic field line crossing the baropause at 45° latitude and 1.1 earth radii. The solid line corresponds to $N_1 = N_2$. For comparison, the dashed lines correspond to $N_2 = 0.5N_1$ and $N_2 = 2N_1$. The baropause temperatures $T_1 = T_2 = 1500$ °K in each case.

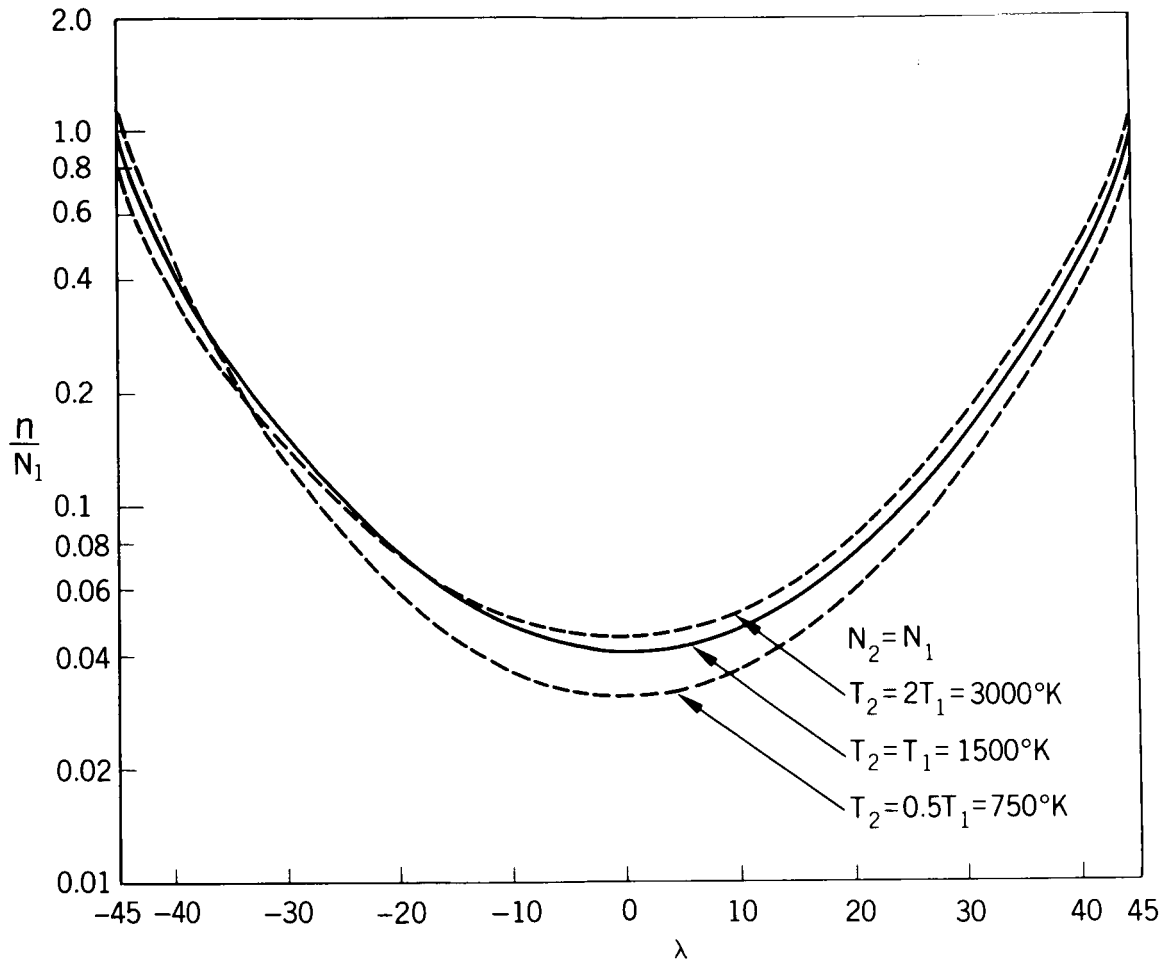

Figure 4–Density ratio n/N_1 versus latitude angle λ along a magnetic field line crossing the baropause at 45° latitude and 1.1 earth radii. The solid line corresponds to $T_1 = T_2 = 1500°K$. For comparison, the dashed lines correspond to $T_2 = 0.5T_1 = 750°K$ and $T_2 = 2T_1 = 3000°K$. The baropause densities $N_1 = N_2$ in each case.